Unusual back-angle scattering and the significance of coupled channels in the ^{60}Ni(α,α') reaction at $E_\alpha = 40$ MeV*

M. B. Lewis, C. B. Fulmer, and D. C. Hensley
Oak Ridge National Laboratory,† Oak Ridge, Tennessee 37830

C. C. Foster, N. M. O'Fallon, and S. A. Gronemeyer
University of Missouri–St. Louis, St. Louis, Missouri 63121

W. W. Eidson
Drexel University, Philadelphia, Pennsylvania 19104

(Received 8 August 1974)

Cross sections were measured for elastic and inelastic scattering of 40.1-MeV α particles from ^{60}Ni over the range $\theta = 153$–$189°$. The 180° cross section for inelastic scattering from the 2^+ excited state at 2.16 MeV was found to be more than an order of magnitude larger than that for the first excited 2^+ state at 1.33 MeV and nearly an order of magnitude larger than that for the elastic scattering. The phase of the angular distribution for the 2.16-MeV level is opposite to that of the 1.33-MeV level, but is the same as the elastic scattering. The data are compared with predictions of compound nucleus and coupled-channel reaction theory. While the compound nucleus reaction mechanism does not account qualitatively for these data, the coupled-channel approach is much more successful and indicates that the absorption term in the optical model potential is determined in a very sensitive way by the back-angle elastic and inelastic scattering.

[NUCLEAR REACTIONS ^{60}Ni(α,α'), $E = 40.1$ MeV; measured absolute $\sigma(\theta)$, $\theta = 153$–$189°$, coupled-channel analysis.]

I. INTRODUCTION

In a variety of recent measurements of back-angle α scattering[1-9] it has been shown that unusually large 180° differential cross sections often characterize the angular distributions. These measurements have generally been made on rather light nuclei ($A \leq 40$) or at rather low bombarding energy ($E \leq 30$ MeV) in which the compound nucleus formation or α-clustering effects are likely to be important if not dominant features in the reaction mechanism.

Recently Trombik *et al.*[10] have extended these back-angle α-scattering measurements to the nickel isotopes, finding no anomalous cross sections in the elastic or inelastic channels for bombarding energies 18–27 MeV. They account for this negative result by the much higher level density in the compound system for these higher mass targets.

However, back-angle scattering measurements offer a sensitive probe for investigating any nuclear reaction model or mechanism. This can be seen in a simple way by presenting the differential cross section in the usual partial wave expansion

$$\sigma(\theta) \propto \left| \sum_l (2l+1) \exp(i\delta_l) \sin\delta_l P_l(\cos\theta) \right|^2 ,$$

where each partial wave l contributes coherently to the total cross section. For forward angles $\cos\theta \sim 1$ and $P_l \sim 1$ for all l, whereas for angles near 180°, $\cos\theta \sim -1$ and $P_l \sim (-1)^l$. The latter condition may result in a severe cancellation of amplitudes depending on the precise value of the phase shift δ_l. Even small defects or omissions in the theoretical description of the reaction may give rise to large discrepancies when compared with back-angle data.

Extreme back-angle α-particle scattering is a particularly attractive test case because it is related to forward-angle heavy ion scattering through comparable momentum transfer, while having important absorptive terms in the optical potential as in the case of heavy ion scattering. In the present work we show that unusual back-angle α scattering does in fact characterize the ^{60}Ni(α,α') reaction at $E_\alpha = 40$ MeV, and that this kind of data can be used to probe the details of nuclear reaction mechanisms.

II. EXPERIMENT

Data were obtained with a beam from the Oak Ridge Isochronous Cyclotron (ORIC) as part of a survey of back-angle α scattering at 40 MeV. The

back-angle scattering facility[11] consists of a magnet and scattering chamber arranged such that the incoming beam is deflected by the magnetic field onto the target foil and back-scattered particles are then deflected by the magnetic field in the opposite direction, away from the beam and toward a detector. The detector is mounted on a movable arm to permit angles from about 150° through and past 180° to be measured.

A position-sensitive detector was used for simultaneous data accumulation over a range of angles. This increased efficiency is needed because the particles are scattered in a reflection mode from the target, which necessitates the use of rather thin target foils, and because the cross sections being measured are small—$\lesssim 1$ μb/sr in some regions. A seven-aperature collimator in front of the position-sensitive detector defined counting geometries at intervals of 1°. The ORIC data handling system[12] was used to accumulate energy spectra. The symmetry of the angular distributions about 180° was used to check the positioning of the detector.

The present ^{60}Ni data were obtained principally with a target foil 3.0 mg/cm^2 thick and 800 μC of beam at each detector angle. In the energy spectra the 2.51-MeV level was poorly resolved from the unresolved doublet of 2.16-MeV 2^+ and 2.29-MeV 0^+ levels. Subsequently a target foil 187-μg/cm^2 thick was used to resolve the doublet at and near 180° where the composite cross section is relatively large. An energy spectrum obtained with the thinner target is shown in Fig. 1. For these data 3800 μC of beam was needed and consequently data with the thinner target do not cover a wide angular range.

The 180° spectrum shown in Fig. 1 has the largest intensity for the 2.16-MeV 2^+ level with much lower intensities for the levels at 2.29 and 2.51. This is in contrast to the 34-MeV forward angle data of Inoue[13] where scattering to the 2.16- and 2.29-MeV levels is of equal intensity and scattering to the 2.51-MeV level is an order of magnitude larger. We note the absence of cross section to the 3^+ state as expected for the excitation of an unnatural parity state by α particles in 180° scattering.

Figure 2 shows angular distributions measured with the 3-mg/cm^2 ^{60}Ni target. At 180° inelastic scattering to the unresolved doublet is more than an order of magnitude larger than the elastic scattering. The data with the thinner target show the doublet to consist of ~80% scattering to the 2.16-MeV level at 180°. The limited amount of higher resolution data show the angular distribution of the 2.29-MeV 0^+ line to be flat near 180°. It may be that a large part of the cross section for the doublet in the minimum at 172° is due to the 2.29-MeV level. Another unusual result of the measurements is the angular distribution minimum at 180° for the first excited state of ^{60}Ni.

Figure 3 compares some of the angular distributions from the present work with forward-angle 43-MeV data of Broek *et al.*[14] The back-angle cross section for inelastic scattering to the two-phonon doublet is as large as at forward angles in the data of Refs. 14 and 13.

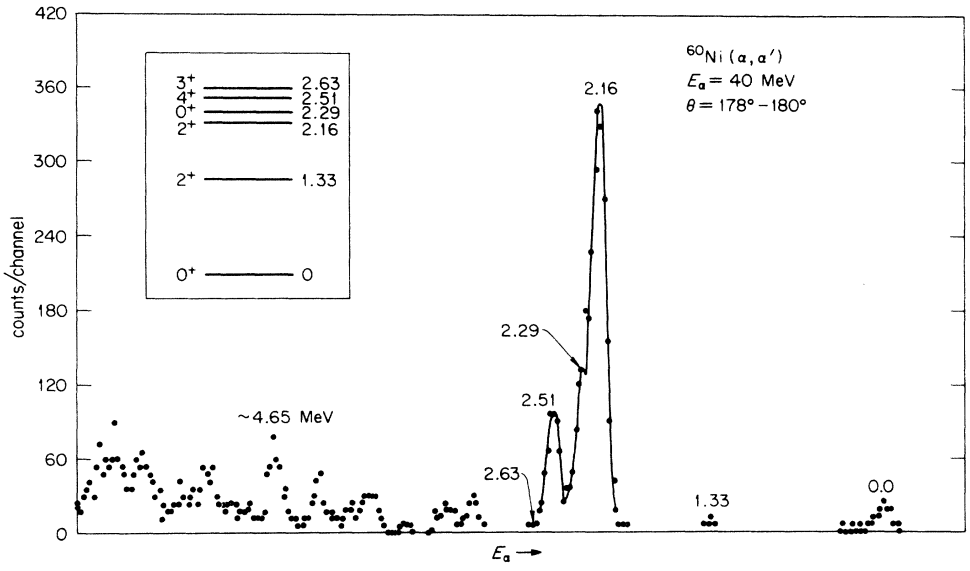

FIG. 1. Energy spectrum of 40-MeV α particles scattered ~180° from ^{60}Ni.

III. ANALYSIS

A. Compound nucleus approach

In order to illustrate the qualitative features which one expects from a compound nucleus approach to the back-angle inelastic scattering problem we have made use of the code DEFSPO.[15] In these calculations the total transmission is parametrized in the manner suggested by Eberhard *et al.*[16]

$$\sum_c T_c = 2\pi \frac{\langle \Gamma^\circ \rangle}{D^\circ} (2J+1) \exp\left[\frac{-J(J+1)}{2\sigma^2}\right],$$

where D° and $\langle \Gamma^\circ \rangle$ stand for the mean spacing and mean width of levels with the lowest possible spin in the compound nucleus, and σ is the average spin cutoff parameter of the nuclei predominantly formed in the decay of the compound system. This leads to a predicted cross section of the form

$$\sigma^J_{cc'} \sim \frac{T_{c'} T_c (1+\delta_{c'c})}{(2J+1)\rho} \exp\left[\frac{J(J+1)}{2\sigma^2}\right],$$

where

$$\rho = 2\pi \langle \Gamma^\circ \rangle / D^\circ$$

and the J values are meant to be those characteristic of the compound system. In DEFSPO the transmission coefficients T_c are calculated from the optical model; the optical model parameters used here are those reported in Ref. 9 and given in Table I. The value used for the spin cutoff

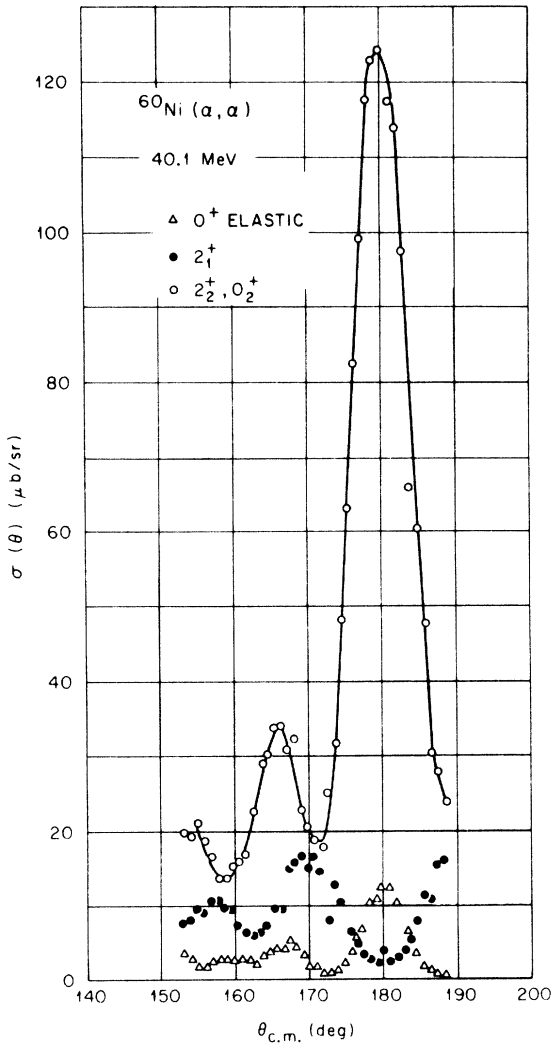

FIG. 2. Back-angle 40-MeV α elastic and inelastic scattering angular distributions for ^{60}Ni.

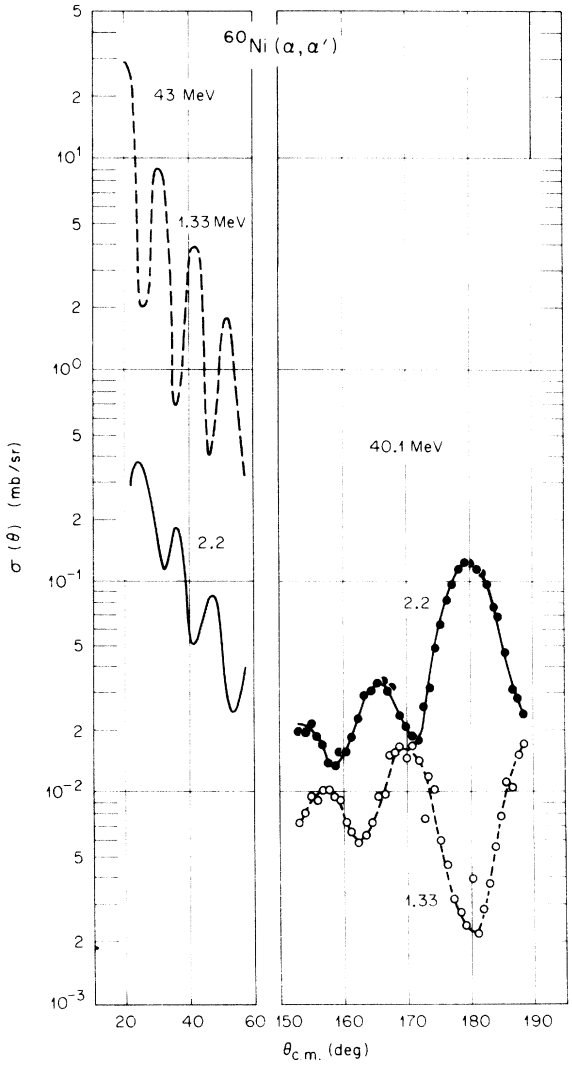

FIG. 3. Forward-angle and back-angle α inelastic scattering angular distributions for ^{60}Ni. The angular distributions labeled "2.2" are for the 2^+ level at 2.158 MeV and the (0^+) level at 2.286 MeV. The forward-angle data are from Ref. 14.

parameter, $\sigma^2 = 25$, is based upon a study by Lu, Vaz, and Huizenga[17] and upon energy dependent relations of Gilbert and Cameron.[18] The level density parameter, $\rho = 10^6$, was chosen to normalize the calculated elastic scattering to agree with the measured value at $\theta = 180^\circ$

The calculated cross sections are given in Fig. 4, and were found to be qualitatively insensitive to variations in σ and ρ. The curves are shown for the elastic and the first three levels of ^{60}Ni. The results show that (a) all curves peak at $\theta = 180^\circ$, (b) the curves for the first and second excited states are nearly identical, (c) the elastic curve has the largest cross section at $\theta = 180^\circ$. We find that each of these qualitative properties predicted by the statistical compound nucleus model is basically inconsistent with the experimental findings.

B. Coupled-channel approach

It was shown by Tamura[19] that the first excited state in ^{60}Ni can be characterized as a one-phonon level while the next three levels resemble a two-phonon triplet with spins 2^+, 0^+, and 4^+, respectively. For this reason we have utilized the code JUPITOR[19] (Karlsruhe version) in order to calculate angular distributions for the elastic, one-phonon, and two-phonon levels in ^{60}Ni.

A two-phonon level cannot be treated by the usual distorted wave Born approximation (DWBA) method, but can be handled in a natural way with a coupled-channel Born approximation treatment (CCBA). In addition, the elastic and one-phonon levels are treated self-consistently in CCBA, but not in DWBA. This consistency results from the use of the procedure that the total wave function is expanded in terms of the excited states Φ_{I_n} of the target as

$$\psi = r^{-1} \sum_{J_n l_n j_n} R_{J_n l_n j_n}(r)[Y_{l_n j_n} \otimes \Phi_{I_n}]_{JM},$$

where R is the radial wave function and Y the spherical harmonic with quantum numbers in the usual notation. Solution of the resulting Schrödinger equation yields the simultaneous solutions for all the nuclear levels in the above expansion. This method is particularly important for back-angle scattering because the elastic scattering wave functions do not necessarily dominate the inelastic wave functions and, as we show below, all the channels are comparably affected by the coupling procedure.

TABLE I. Optical model parameters for the $\alpha + ^{60}$Ni system for $E_\alpha \approx 50$ MeV from Ref. 9.

V (MeV)	W_D (MeV)	r_R (fm)	r_I (fm)	a_R	a_I
97.0	45.3	1.48	1.39	0.586	0.402

The initial CCBA calculations used the optical model parameters given in Table I. The reduced matrix element or $\beta = 0.20$ was taken[20] as the coupling parameter, and the first two excited levels of ^{60}Ni were coupled to the ground state. The results of these distorted wave calculations indicated that the forward-angle predictions depend most on the real part of the optical model potential while the back-angle predictions are much more sensitive to the absorption part. Thus the search routine in the code JUPITOR was found to be useful for determining the preferred shape and magnitude of the imaginary part of the optical model potential which could be used in the coupled-channel calculations.

To illustrate the sensitivity of the back-angle scattering to the one-phonon level of ^{60}Ni when coupled to the zero-phonon (elastic) and two-phonon levels, we have plotted in Fig. 5 the 180° cross section as a function of the imaginary surface term of the potential. It is of interest to note that either an enhancement or hindrance of the back-angle cross section may result from various choices of absorptive potential.

In general one would like to include as many re-

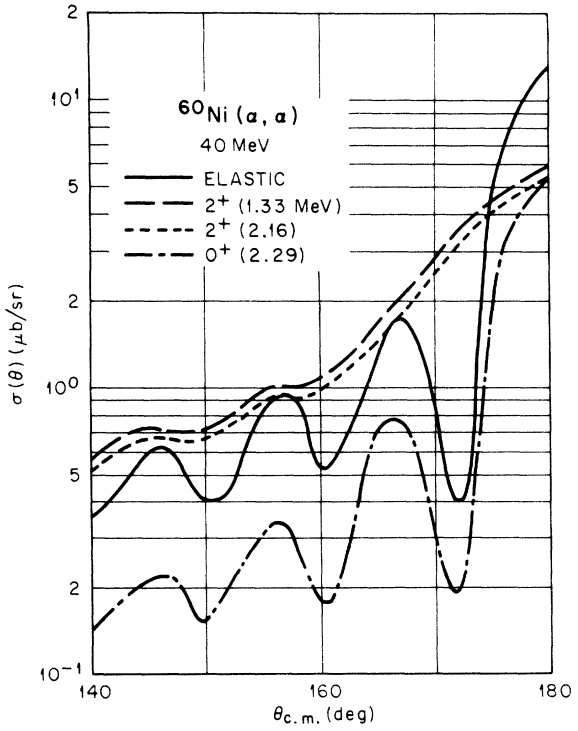

FIG. 4. Calculated angular distributions based on a compound nucleus reaction model (see text).

action channels as possible in a calculation of this kind. However, we found that with the present code, 0_0^+-2_1^+-2_2^+-0_2^+ coupling was the maximum allowed with 40-MeV α particles on ^{60}Ni in which a minimum of about 40 partial waves were needed for convergence[21] at $\theta = 180°$. The above coupling notation refers to J^π subscripted by the phonon number. Since we showed that large cross sections are due mostly to 2_2^+, and since the computer time increases rapidly with the number of channels, most searches were made with only 0_0^+-2_1^+-2_2^+ coupling. Comparisons of 0_0^+-2_1^+-2_2^+-0_2^+ cases with 0_0^+-2_1^+-2_2^+ usually showed that the additional 0_2^+ coupling had small effects upon the 0_0^+, 2_1^+, and 2_2^+ channels.

In the calculations other parameters were held fixed even though their values are not well known. Uncertainties in these parameters do not alter the conclusions in this paper except as noted in c.

(a) Coupling (deformation) parameters β: The deformation parameters β_2 for the excitation of the one-phonon level ($J^\pi = 2^+$ $E = 1.3$ MeV) in ^{60}Ni is rather well established $\beta_2 \approx 0.20$.[20] However, the reduced matrix element $\langle 2_2^+ \| Q \| 2_1^+ \rangle$ which characterizes the two-phonon purity of the second quadrupole level in ^{60}Ni is not known. We have taken the 2_2^+ level as 50% two-phonon. Following the procedure suggested by Tamura,[19] $\beta(2_1 \to 2_2) = \beta_2 A_{2\mathrm{ph}} = 0.14$ where $A_{2\mathrm{ph}}$ is the two-phonon amplitude. In addition $\beta(0_0 \to 2_2) = [\beta_2 \beta(2_1 \to 2_2)]^{1/2} = 0.17$.

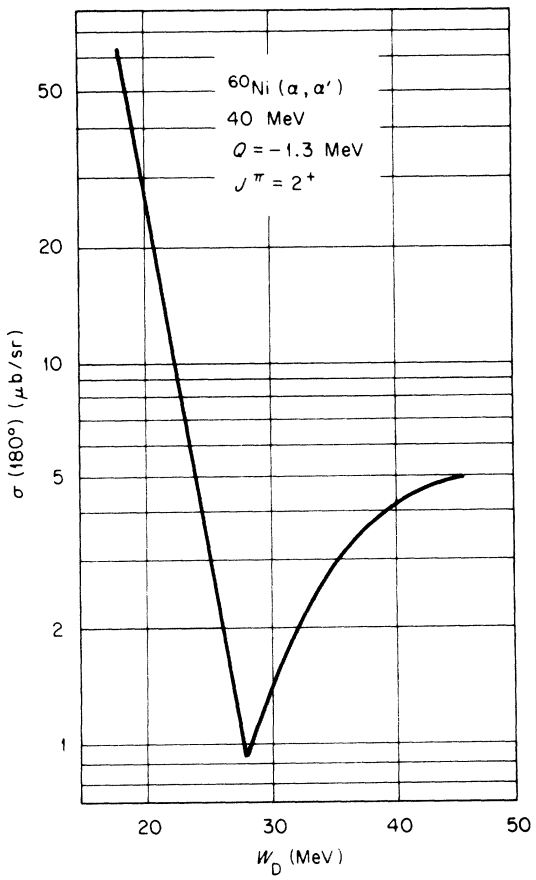

FIG. 5. Coupled-channel predictions of 40-MeV α inelastic scattering to the first excited state of ^{60}Ni as a function of absorption well depth of the potential.

TABLE II. Parameters for the absorptive part of the potential without volume absorption used in the coupled-channel calculations for ^{60}Ni. Parameters for the real well are given in Table I.

	W_D (MeV)	r_I (fm)	a_I
Initial value	45	1.39	0.40
Final value	36	1.35	0.39

(b) Channel potential "adjustment" factors $W_c(n)$: The coupled equation for each channel n contains an imaginary potential written as a product $W_n = WW_c(n)$ so that the potential in each channel can be varied by varying $W_c(n)$. Tamura[19] suggested that $W_c(n)$ should be slightly larger than unity for the inelastic channels in order to compensate for the neglect of including all other inelastic channels in the calculation. We have assumed that $W_c(n) = 1.2$ and 1.4, respectively, for the 2_1^+ and 2_2^+ channels.

(c) The one-phonon amplitude in the two-phonon wave function was taken to be zero since the $B(E2)$ $2_2^+ \to 0_0^+$ is known experimentally to be very small.[22] If this small experimental value is not mostly due to the multiple-phonon character of the 2.2-MeV level in ^{60}Ni, our use of the JUPITOR code is not appropriate. In other words we assume that the 2.2-MeV peak can be characterized as a sum of two-phonon and higher-order phonon levels, and to a first approximation the inelastic scattering cross section is determined by the two-phonon component.

A number of searches for optimum fits to the back-angle data were performed with and without the forward-angle scattering data[14] included. Starting with the parameters given above the searches consistently resulted in smaller magnitude and extent for the imaginary well. This result

TABLE III. Volume and surface well depths of the potential obtained in coupled-channel fits for ^{60}Ni data. The values of the geometry terms and real well depth in Table I were held constant.

	W (MeV)	W_D (MeV)
Initial value	20	20
Final value	40	−10

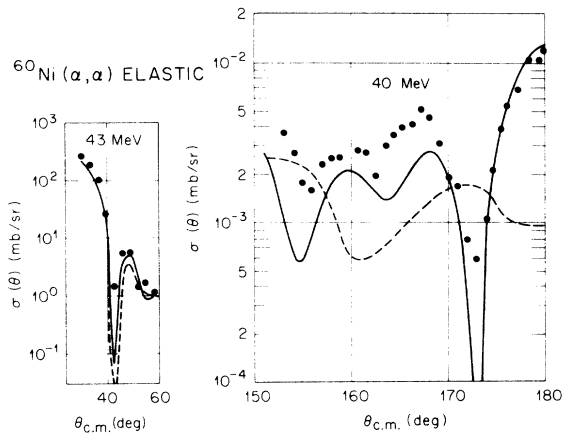

FIG. 6. Coupled-channel fits for forward-angle and back-angle ^{60}Ni elastic scattering data. The forward-angle data are from Ref. 14. Parameters are listed in Table I for the dashed curves; for the solid curves this potential was modified by using the final value absorption well depths listed in Table III.

is consistent with that found by Tamura.[19] Typical results are listed in Table II. When we generalized the potential to include both volume and surface potential shapes, the preferred combination was a "depleted surface" potential, i.e., a negative sign for the derivative term as shown in Table III.

Both the trends in Table II and Table III are consistent in that they show the need for reducing the "surface" reaction contribution to the imaginary potential.

The "depleted surface" potential is interesting not only because it fits the data better than conventional potentials without changing r_I and a_I, but also because it shows more directly the physical origin of the imaginary potentials. Since the one-phonon 2_2^+ excitation takes place at the nuclear surface, it contributes to the surface imaginary optical model term in the potential. When the 0^+-2_1^+ coupling is explicitly included in a coupled-channel calculation, this surface potential must, consequently, be decreased relative to the remainder of the imaginary potential.

Fits to the data with the final values in Table III and assumptions (a), (b), and (c) are shown as solid curves in Figs. 6 and 7. In general, the theoretical predictions reproduce the measured cross sections much better in the forward than in the backward hemisphere. The dashed curve represents the coupled-channel prediction when the original parameters from Table I are used. The forward-angle predictions for the ground and one-phonon levels are not seriously affected by changes in the imaginary potential. On the other hand the back-angle predictions as shown in Figs. 6 and 7 are very sensitive to the choice of absorptive po-

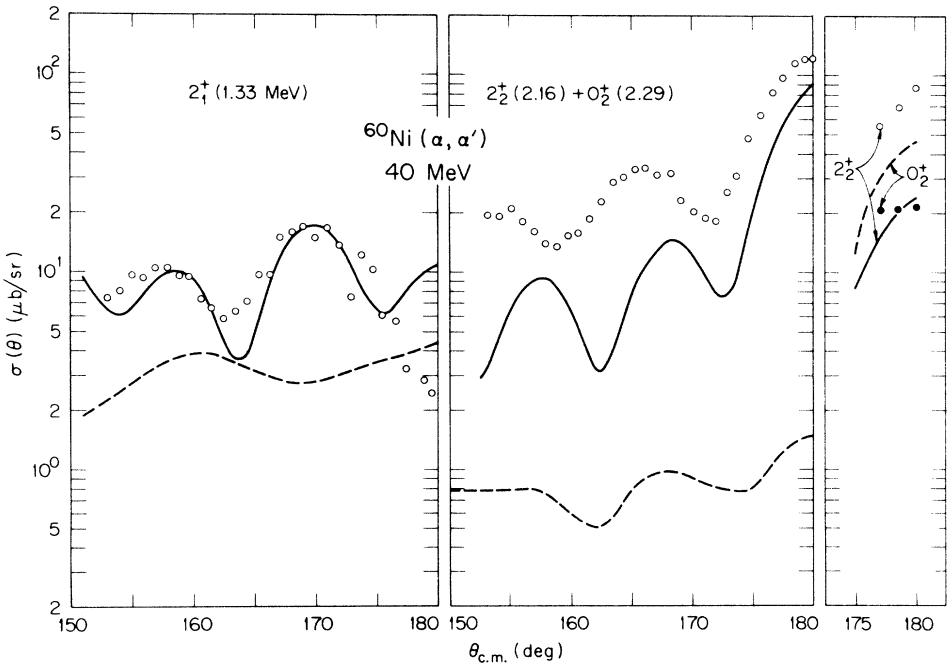

FIG. 7. Coupled-channel fits for back-angle ^{60}Ni inelastic scattering data. Parameters are listed in Table I for the dashed curves; for the solid curves this potential was modified by using the final value absorption well depths listed in Table III.

tential.

While the new parameters improve significantly the fits to the inelastic scattering data, particularly near 180°, discrepancies remain. A contribution of a few μb/sr from compound nucleus cross sections would be consistent with the present data and could account for the absence of very deep minima in the measured back-angle cross section. More extensive searches on the other parameters r_I, a_I, $\beta's$, $W_c(n)$ were not found to substantially improve the fits.

IV. CONCLUSIONS

We have attempted to approach back-angle scattering in a more general way by suggesting that the differential cross sections observed are related to details of the nuclear reaction mechanism. With this in mind, one should expect that strange back-angle differential cross sections might be observed in various scattering and reaction experiments: light ion, heavy ion, low energy, and high energy. Whereas the low energy-light target combination is likely to be influenced by the formation of intermediate compound nuclear states, the higher energy-heavier target combination should manifest a characteristic back-angle structure due to the exact manner in which the incident flux is absorbed near the nuclear surface.

The theoretical method of coupled channels is particularly appropriate for the latter case since it is the open reaction channels which determine the absorptive part in the optical model potential. In the ^{60}Ni(α, α') reaction at $E_\alpha = 40$ MeV we found that small variations in the absorptive potential had only a small effect upon the compound nucleus predictions for back-angle scattering. However, the direct or two-step elastic and inelastic scattering predictions were quite sensitve to the choice of absorbing potential, particularly when the reaction channels are coupled. The $W_D = -10$ MeV correction to the volume absorption given in Table III affects the absorption at the nuclear surface as does, say, an l-dependent absorptive potential. It is not entirely a substitute, however, for l dependency for the following reasons: The l or J dependency[23] suppresses all of the high angular momentum components in the partial wave expansion. This has the effect of increasing the back-angle cross sections for almost all levels without significant changes in the oscillatory structure. In contrast, the "depleted surface" potential introduced here has the effect of slightly suppressing only those partial waves near the value $l \sim kR$, and this affects the angular distributions in a unique way as we have shown. Unless the coupled-channel calculations are complete, there remains a physical justification for l- or J-dependent absorption as discussed in Ref. 23. Complex or heavy ions, which are expected to be strongly absorbed, would be good candidates for back-angle studies.

An important consideration in the compound nucleus coupled-channels problem is the energy region where the transition between predominantly compound and direct reaction is supposed to occur. A ^{58}Ni(α, α') excitation function for 180° scattering from ≈15–30 MeV has been measured by Sewell *et al.*[9] These data could not be fitted with the optical model (using parameters which fit the scattering data forward of 140°), but the data showed no large compound nucleus resonances. We found in the present coupled-channel calculations using parameters in Table III that we were likewise not able to fit the low energy data, underestimating it similarly as in the calculations in Ref. 9. It would therefore be important to measure the back-angle excitation function between 30–40 MeV for the α+Ni system and determine what optical potential form is necessary to fit this kind of data.

Since the back-angle inelastic scattering is very sensitive to the absorptive potential in CCBA, it is not surprising that we have not been able to fit the relative cross sections to the 2_2^+ (2.16-MeV) and 0_2^+ (2.29-MeV) levels (see Fig. 7). The calculations are incomplete in at least two ways: (a) We have not coupled the two-phonon levels to the three-phonon levels. (b) There is no correction for l dependence of the absorptive potentials. It is hoped that we have presented support for future theoretical work in this area.

ACKNOWLEDGMENTS

The authors wish to thank R. G. Rasmussen and D. Bickford for assistance in taking and processing the data; the operations crew of the Oak Ridge isochronous cyclotron for their willing and able service; the Washington University Physics Department for the use of the back-angle magnet; and the Oak Ridge Associated Universities for travel funds.

---

*Research supported in part by the National Science Foundation.

†Operated by Union Carbide Corporation for the U. S. Atomic Energy Commission.

[1] G. Gaul, H. Lüdecke, R. Santo, H. Schmeing, and R. Stock, Nucl. Phys. A137, 177 (1969).

[2] H. Oeschler, H. Schröter, H. Fuchs, L. Baum, G. Gaul, H. Lüdecke, R. Santo, and R. Stock, Phys. Rev. Lett.

28, 694 (1972).
[3]A. Bobrowska, A. Budzanowski, K. Grotowski, L. Jarczyk, S. Micek, H. Niewodniczanski, A. Strzalkowski, and Z. Wrobel, Nucl. Phys. A126, 361 (1969).
[4]A. Budzanowski, A. Dudek, R. Dymarz, K. Grotowski, L. Jarczyk, H. Niewodniczanski, and A. Strzalkowski, Nucl. Phys. A126, 369 (1969).
[5]P. David, J. Debrus, H. Mommsen, and A. Riccato, Nucl. Phys. A182, 234 (1972).
[6]H. Schmeing and R. Santo, Phys. Lett. 33B, 219 (1970).
[7]*Proceedings of the Symposium on Four Nucleon Correlations and Alpha Rotator Structures, Marburg, Germany, 1972*, edited by R. Stock (unpublished), and literature cited therein.
[8]R. Stock, G. Gaul, R. Santo, M. Bernas, B. Harvey, D. Hendrie, J. Mahoney, J. Sherman, J. Steyaert, and M. Zisman, Phys. Rev. C 6, 1226 (1972).
[9]P. T. Sewell, J. C. Hafele, C. C. Foster, N. M. O'Fallon, and C. B. Fulmer, Phys. Rev. C 7, 690 (1973).
[10]W. Trombik, K. A. Eberhard, G. Hinderer, H. H. Rossner, A. Weidinger, and J. S. Eck, Phys. Rev. C 9, 1813 (1974).
[11]J. C. Hafele, C. Chatlos, and C. C. Foster, Bull. Am. Phys. Soc. 16, 830 (1971); J. C. Hafele and F. B. Shull, Washington University Department of Physics Technical Report, September 1970 (unpublished).
[12]C. D. Goodman, C. A. Ludemann, D. C. Hensley, K. Kurz, and E. W. Anderson, IEEE Trans. Nucl. Sci. NS-18, (1), 323 (1971); D. C. Hensley, *ibid.* NS-20, (1), 334 (1973).
[13]M. Inoue, Nucl. Phys. A119, 449 (1968).
[14]H. W. Broek, T. H. Braid, J. L. Yntema, and B. Zeidman, Phys. Rev. 126, 1514 (1962).
[15]W. I. van Rij, private communication.
[16]K. Eberhard, P. Von Brentano, M. Bohning, and R. O. Stephen, Nucl. Phys. A125, 673 (1969).
[17]C. C. Lu, L. C. Vaz, and J. R. Huizenga, Nucl. Phys. A197, 321 (1972).
[18]A. Gilbert and A. G. W. Cameron, Can. J. Phys. 43, 1446 (1965).
[19]T. Tamura, Rev. Mod. Phys. 37, 679 (1965); Oak Ridge National Laboratory Report No. ORNL-4152, 1967 (unpublished); private communication. The Karlsruhe version of the code JUPITOR used in the present work is a modification by H. Rebel and G. W. Schweimer.
[20]S. Raman, Nucl. Data B2, (No. 5), 41 (1968).
[21]In other words, the calculation was "stable" for small changes in the integration radius, mesh size, and the maximum number of partial waves used. Such "stability" problems have been discussed in detail by R. R. Doering, A. I. Galonsky, and R. A. Hinrichs, Michigan State University Report No. MSUCL-61, 1972 (unpublished).
[22]D. M. van Patter, E. J. Hoffman, T. Becker, and P. A. Assimakopoulos, Nucl. Phys. A178, 355 (1972).
[23]J. G. Cramer, K. A. Eberhard, J. S. Eck, and W. Trombik, Phys. Rev. C 8, 625 (1973).